Research scanning polarimeter and airborne usage for remote sensing of aerosols

Brian Cairns[*a], Edgar E. Russell[b], Joseph D. LaVeigne[b], Philip MW. Tennant[b]
[a]Dept of Applied Physics and Applied Mathematics, Columbia University, New York, NY 10025
[b]SpecTIR[†] Corporation, Goleta, CA 93117

ABSTRACT

Accurate multi-spectral, multi-angle polarimetric measurements are a key remote sensing tool for the determination of the burden and microphysical properties of atmospheric aerosols and, as an adjunct, for the correction of these atmospheric effects in spectroradiometric remote sensing applications. This paper describes the performance of the Research Scanning Polarimeter (RSP), provides examples of using the RSP for aerosol remote sensing, and assesses the potential synergy between spectroradiometric and polarimetric measurements.

Keywords: Polarimetry, aerosol characterization, airborne remote sensing, hyperspectral imaging, atmospheric correction

1. INTRODUCTION

An inherent problem in remote sensing applications is the variation of the intervening atmosphere during imaging and spectro-radiometric measurements. Constituent gases and aerosols in the optical viewing path of remote sensors change temporally and with range, illumination, and viewing angle. These atmospheric constituents affect images and contaminate the spectral signatures of objects being observed. Correcting for the intervening atmospheric is typically done via post-processing of recorded data, using ground based photometric illumination measurements, and applying generalized atmospheric-model corrections via "standardized" software to derive the final "reflectance" data set. These processes provide some correction, but cannot precisely account for the specific effects of the actual aerosol that is present. The nature and magnitude of these effects depends strongly on the aerosol characteristics in the viewing path.

What is needed is a sensor (polarimeter) capable of measuring the scene polarized radiance to accurately characterize atmospheric aerosols and determine the concentration (optical depth), size distribution and chemical composition (refractive index) of the aerosols in the optical path. The use of such a sensor in tandem with imaging and spectro-radiometric measurements will allow for the suitable correction of datasets for the effects of intervening atmospheric aerosols.

This paper describes SpecTIR's RSP design and performance, aerosol detection and characterization processes and performance, and results obtained using the RSP with simultaneous hyperspectral imaging. Potential opportunities and enhancements for the future are discussed in the final sections.

1.1 Background

The remote sensing of tropospheric aerosols relies on reflected solar radiation that is, in general, polarized and contains embedded information about the intrinsic nature of aerosol particles as well as the underlying surface. Some of this information is accessible through standard remote sensing techniques that utilize changes in the intensity of reflected solar radiation with wavelength and viewing geometry. However, a complete picture of the aerosol microphysical state is only available through the measurement and analysis of the spectral and angular polarization signature of the reflected radiation. There are also instrumental calibration advantages in making polarization measurements. The accuracy of aerosol retrievals using intensity-only measurements is largely determined by the **absolute** radiometric calibration. In contrast, it is only necessary to provide an accurate **relative** calibration to ensure very high polarimetric accuracy. This has allowed polarimetric remote sensing of aerosols to be performed with an accuracy that allows the intrinsic information content of polarization measurements to be realized.

[*] phone 212 678-5625; bcairns@giss.nasa.gov
[†] phone 805 961-0500; erussell@spectir.com; jlaveigne@spectir.com; ptennant@spectir.com; www.spectir.com

SpecTIR, with internal investment and under contract to Columbia University, has developed and operated an airborne RSP for atmospheric studies under the sponsorship of the NASA Goddard Institute for Space Studies (GISS) science teams. The RSP served as the prototype for the UnESS spaceflight instrument proposed for International Space Station observations and, more recently, the RSP has demonstrated compliance for the mission of the NPOESS aerosol polarimetry sensor and the retrievals of aerosol and cloud environmental data records. The RSP has demonstrated that a carefully designed polarimetric instrument can make measurements of polarization with an accuracy that allows the very high information content regarding aerosol properties to be realized. The scientific requirements for the polarimetric measurements are satisfied by the RSP through its high measurement accuracy, a wide range of viewing angles measured and sampling of the spectrum of reflected solar radiation over most of the radiatively significant range.

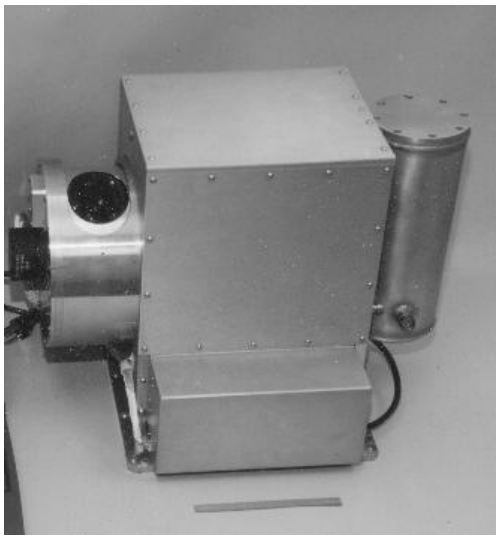

Figure 2.1: RSP; Scanner on the left and Dewar on the right

2. REARCH SCANNING POLARIMETER

The RSP (Figure 2.1) measures scene linear polarization at four polarization azimuths and in nine spectral bands simultaneously. Scene viewing begins with the polarization-compensated scanner collecting a swath of contiguous instantaneous field of view (IFOV) samples (sectors) over a scene field of view (FOV) range of over 90°. The scanner output is directed towards three pairs of boresighted optical assemblies that provide the IFOV definition, polarimetric and spectral separation, and relay the resultant optical beams onto pairs of photodiodes. The individual optical assemblies are mounted rotated by 45° in azimuth to each other and in this manner scene linear polarization components are measured simultaneously at azimuths of 0° and 90° and at 45° and 135°. Each paired optical assembly services three spectral bands for a total of nine spectral bands, and this provides 36 simultaneous signal measurements for each IFOV. In this manner, "false polarization", introduced from scene spatial variations in instruments that lack such simultaneity provided by the RSP design, is avoided. This configuration provides simultaneous scene measurements of the Stokes parameters I, Q and U, Q by one optical assembly of a pair, U by the other, and I independently by both.

With the RSP oriented to scan in an along-track mode, as the aircraft travels, the same area on the ground is seen from multiple view angles. During the course of a scan, scene samples, calibration samples and dark reference samples are collected.

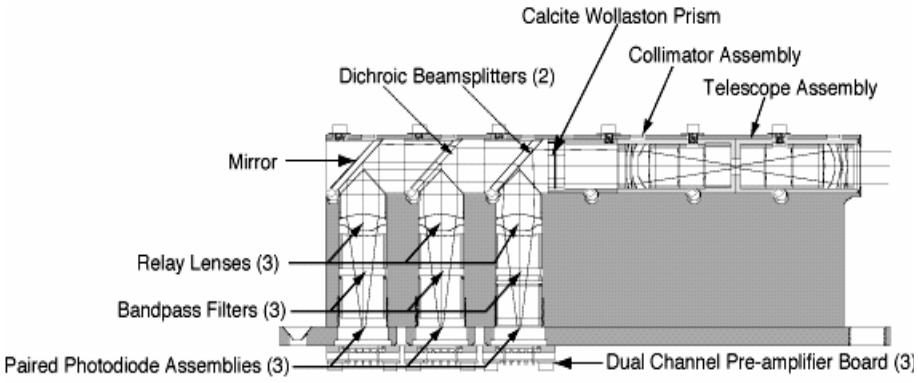

Figure 2.2: RSP VNIR Optical Assembly

Figure 2.2 is a side view of a visible/near infrared (VNIR) telescope optical assembly, showing telescope and collimator assemblies, Wollaston prism, dichroic beamsplitters and mirror, relay lenses, bandpass filters, and protective windows. Short wave infrared (SWIR) optical assemblies are functionally similar to that of the VNIR except for optical material changes required for different spectral region and detectors are housed in a vacuum vessel to facilitate cooling.

In the VNIR spectral region blue enhanced silicon photodiodes provide scene measurements in six spectral bands centered at 410, 470, 555, 670, 865 and 960nm. Similarly, in the SWIR, HgCdTe detectors support measurements in three spectral bands centered at 1590, 1880 and 2250nm. To achieve optimal noise performance, the SWIR detectors

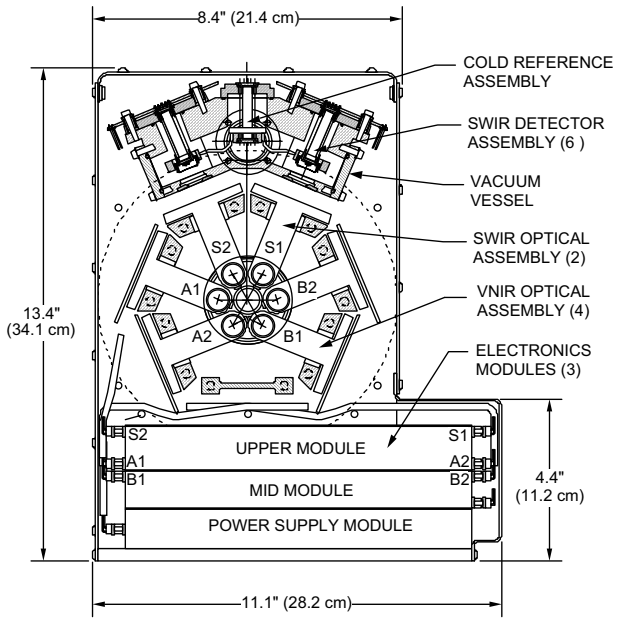

Figure 2.3: Cutaway View of RSP

are cooled to less than <165K using a dewar of liquid nitrogen.

Figure 2.3 is a cutaway end view of the RSP showing the three pairs of optical assemblies (S1/S2, A1/A2, B1/B2) used for simultaneous polarization measurements. Dual-channel preamplifiers are located near each detector pair and the rest of the RSP electronics is contained within three stacked, internally interconnected modules. The electronics provides: the amplification of the signals detected by the 36 detector channels and the sampling and 14-bit analog-to-digital conversion of the resultant signals. Data are stored each scan from 214 sectors (including scene, calibrator and dark reference sectors together with instrument status data) and transmitted to a computer for storage. The average data rate is 20 kbytes/sec for readout of the 36 signal channels and status data for a scan rate of 71.3 rpm. This scan rate results in an IFOV dwell time of 1.875 msec and yields contiguous (scan line-to-line) coverage at nadir for an aircraft traveling at a V/H ratio of 0.017 sec^{-1}.

2.1 RSP calibration and performance

Overall RSP performance is reliant on the sensor being fully characterized during the fabrication and assembly process and the availability of calibrated data every scan from the inflight calibrator. RSP performance is summarized in Table 2.1.

Inflight Polarimetric calibration: The inflight polarimetric calibrator (patent pending), see Figure 2.4, permits accurate relative responsivity measurement of channels measuring orthogonal polarization components that is essential for maintaining long-term polarimetric accuracy. Scene earthshine is reflected through a polarization scrambler consisting of birefringement wedges that spatially vary the polarization state across the apertures of all six optical assemblies and effectively produce near 0% polarized output. The polarimetric calibration measurements are collected each scan by sequential viewing of the inflight calibrator. This implementation requires no moving parts other than normal scanning motion.

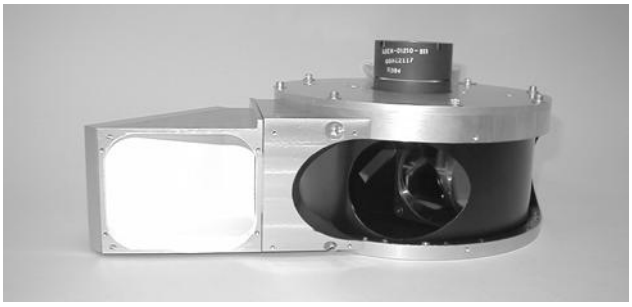

Figure 2.4: RSP Scanner with Inflight Calibrator on the left

Channel Dark Values: Knowledge of channel dark values is essential for accurate remote sensing of aerosols since they directly affect signal determinations. Accurate determination of dark levels is particularly critical for polarimetric measurements due to the high polarimetric accuracy requirements. All RSP signal channels are simultaneously dc-restored during the scanner backscan where the scanner views effectively a zero-radiance zone. Multiple dark samples for inclusion in the data file are collected each scan both before and after the dc-restoration while viewing the zero-radiance zone.

Instrument Calibration: The RSP undergoes characterization including calibration during the fabrication cycle at various sub-assembly levels and at final assembly. Characterization uses a standard laboratory radiometric, spectrometric and field of view test equipment together with specialized equipment for the polarimetric calibrations[1]. Solar-illuminated Spectralon™ viewed with and without a polarization scrambler is used preflight and/or post-flight for verifying polarimetric calibration stability. The redundant measurements of intensity in each spectral band by the paired optical assemblies allows constant monitoring of instrument stability. The long-term stability is further

enhanced by the use of Wollaston prisms for the polarization separation and spectral filters fabricated with ion-assisted deposition for the spectral definition.

Table 2.1: Research scanning polarimeter performance summary

Parameter	Performance
Polarization Accuracy (%)	<0.2
Radiometric Accuracy (%)	<5.0
Dynamic Range	$>10^4$
Signal-to-Noise Ratio	>2000 (with R=0.3)
Spectral Characteristics	See adjacent table
Field of View	$>90^O$
Instantaneous FOV	14 mrad
Photodiode Detector Type: • Visible/NIR • Shortwave IR (temperature)	 Silicon HgCdTe (165K)
SWIR Detector Cooling	LN_2 dewar
Data Rate	<20 kbytes/sec
Size, W x L x H (cm)	40 x 64 x 34
Mass (kg)	<20
Power (watts)	<20 w/o heaters

Band ID	λ_c (nm)	$\Delta\lambda$ (nm)	Wavelength Type	Purpose
V1	410	27	Visible	Aerosol Retrieval
V2	470	20	Visible	Aerosol Retrieval
V3	555	20	Visible	Aerosol Retrieval
V4	670	20	Visible	Aerosol Retrieval
V5	865	20	Near-IR	Aerosol Retrieval
V6	960	20	Near-IR	H_20 Vapor Detection
S1	1590	60	Shortwave-IR	Aerosol Retrieval
S2	1880	90	Shortwave-IR	Cirrus Cloud Screen
S3	2250	130	Shortwave-IR	Aerosol Retrieval

3. AEROSOL REMOTE SENSING

The principal difficulty in retrieving aerosol loadings and microphysical properties using passive remote sensing measurements over land surfaces is the significant spectral and spatial variations in the observed intensities that are caused by the land surface. Over the ocean this spectral contrast is less of a problem and can be minimized by using near infrared (NIR) bands. However, the variability in aerosol microphysical properties is sufficient that extrapolation of aerosol estimates to the visible from the NIR using measurements from a single view are not always sufficiently accurate, even over the ocean, because the actual aerosol properties may be significantly different from those that are assumed in the extrapolation. For example, corrected radiances for ocean color applications can become negative because of errors in extrapolating NIR measurements to the blue/UV.

There are therefore two problems associated with aerosol remote sensing. The first is correctly adjusting the retrieval for surface properties. The second is quantifying, reducing, or eliminating the non-uniqueness present in retrieving aerosols properties from remotely sensed polarized radiances.

3.1 Over land

We will discuss the problem of eliminating the surface contribution to aerosol retrievals in the context of aerosol retrievals over land. This is because for the majority of oceans the spectral albedo can be parameterized as a function of wind speed and chlorophyll concentration and these parameters can be retrieved as part of the aerosol retrieval providing spectral bands are appropriately chosen.

Over land the unique and highly variable spectral signatures of land surfaces and their rapid spatial variations are of considerable value in geological prospecting and crop identification and evaluation [2], but present a problem in determining the aerosol load above them. The polarized light reflected by surfaces may also be of use in remote sensing of the surface, being indicative of its roughness, or in the case of vegetation its leaf inclination distribution [3]. It is believed that this polarization is generated at the surface interface and this hypothesis has been used to develop theoretical models [4] for the polarized reflectance of vegetation and of bare soils. The fact that most surface polarization is generated at the surface interface and that the refractive index of natural targets varies little within the spectral domain of interest suggests that surface polarized reflectance will be spectrally neutral.

If this is the case, then the use of a measurement at a sufficiently long wavelength that the aerosol load is negligible could be used to characterize and correct for surface polarization effects at the shorter wavelengths. Such an approach has also been suggested for use with intensity measurements [5] based on the observation that the surface reflectance at 450 and 670nm is correlated with the reflectance at 2250nm for many surface types. The shorter wavelengths can then be used to estimate the aerosol load and microphysical properties, for example size and refractive index. A theoretical examination of such an approach based on the assumption that the surface polarized reflectance is spectrally neutral has been performed elsewhere [6].

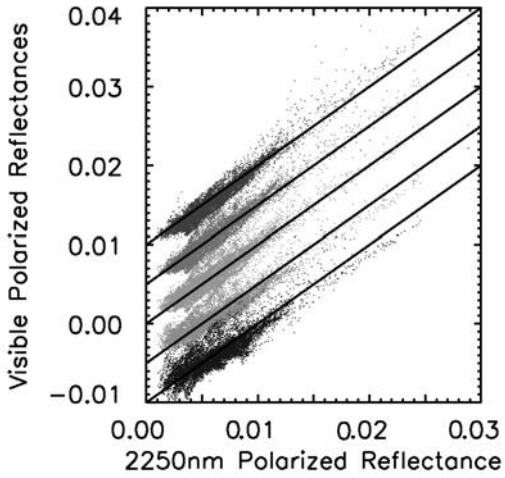

Figure 3.1. RSP measurements that were atmospherically corrected based on simultaneous MFRSR measurements. Symbols and lines are offset to allow different bands to be distinguished. Polarized reflectances at 2250nm plotted against polarized reflectance measurements at 410, 470, 555, 670 and 865 nm (ordered from bottom to top) where the solid lines in are the 1:1 line.

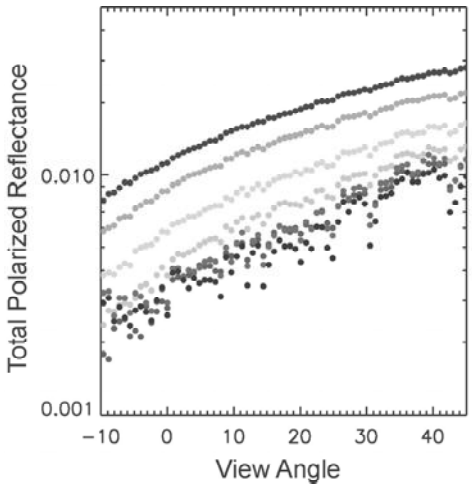

Figure 3.2 RSP measurements of polarized reflectance at 410, 470, 555, 670, 865, 1590 and 2250 nm (ordered from top to bottom respectively) over Pomona Golf Course.

Here we present RSP measurements that demonstrate the spectral variation of the surface polarized reflectance for a range of natural surfaces. The RSP instrument counts were corrected for dark current and reduced to calibrated reflectance. These reflectance measurements contain contributions from both the surface and the atmosphere. The atmospheric contribution was well characterized by sun photometer measurements that provide accurate estimates of aerosol optical depth and allow a plausible aerosol microphysical model to be inferred. The atmospheric reflectance was then calculated using a vector adding/doubling code [7, 6]. The model atmosphere that is used consists of a two layer atmosphere with a pure molecular layer above the aircraft and an aerosol layer mixed with the remaining molecular contribution below the aircraft. The vertical distribution of scattering properties is reasonable for the suppressed boundary layer that was observed and the aerosol properties were defined by the MFRSR measurements. The calculated atmospheric reflectance was then used to correct the RSP measured reflectances so that they provide a reasonable estimate of the surface reflectance [8].

In Fig. 3.1 we show scatter plots of the atmospherically corrected RSP polarized reflectance. The measurements come from a 4km segment of flight track and represent a range of scattering geometries and surface types with approximately 20,000 measurements at each wavelength. The 2250 nm surface polarized reflectance is plotted against the 410, 470, 555 670 and 865 nm surface polarized reflectance. The solid lines are a 1:1 line. As can be seen the measurements are strongly clustered about these lines that are what is theoretically predicted based on our understanding that most of the polarized reflectance from surfaces is generated at the interface and is therefore determined mostly by the real refractive index of the material. Since the real refractive indices of soils and leaves show only weak spectral variation the polarized reflectance also shows weak spectral variation as is apparent in Fig. 3.1.

The approach to aerosol retrievals over land that we will now examine uses the fact that although natural surfaces are spectrally neutral they show considerable contrast at the spatial resolution of the RSP instrument (40 m). Under most conditions the aerosol accumulation mode contribution to the polarized reflectance at 2250 nm is small and so a measurement in this spectral band can be considered to be essentially a measurement of the surface. Since multiple interactions between the atmosphere and surface tend to depolarize scattered light the observed polarized reflectance can then be modeled by the equation

$$R_P^{Obs}(\lambda) = R_P^{Atm}(\lambda) + T^{Dir}(\lambda) R_P^{Obs}(2250). \quad (1)$$

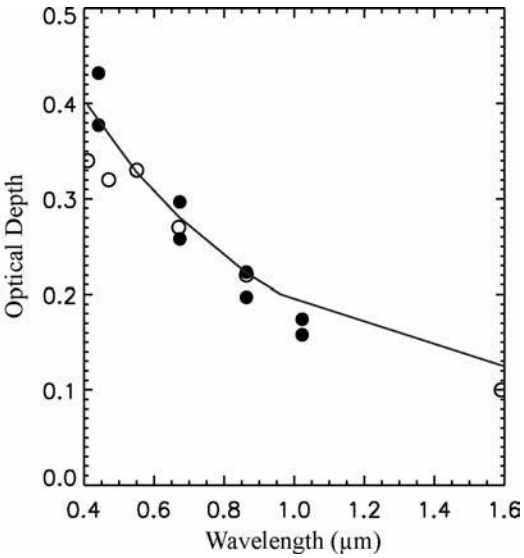

Figure 3.3. RSP optical depth estimates over Pomona Golf Course using simple approach (open symbols) and using iterative search (line). Filled symbols are optical depths measured by a CIMEL instrument at JPL thirty minutes before and after the RSP measurements.

The atmospheric polarized reflectance varies smoothly with view angle location and generally with spatial location. In contrast the surface polarized reflectance varies significantly with spatial location and the observed polarized reflectance shows this coherently in all bands as is shown in Figure 3.2.

This variability can be used to estimate the direct beam transmission along the sun-earth-sensor path and consequently the aerosol optical depth. The apparent atmospheric polarized reflectance is defined to be

$$R_P^{App}(\lambda) = R_P^{Obs}(\lambda) - T^{Dir}(\lambda) R_P^{Obs}(2250). \qquad (2)$$

The aerosol optical depth is then determined by finding the direct beam transmission that minimizes the angular variability in the apparent atmospheric polarized reflectance compared with a smooth polynomial. This approach works well for spectral bands at wavelengths longer than 500 nm as is shown in Fig. 3.3.

At shorter wavelengths, the variability signal is smaller, adjacency effects become more important and the assumption that diffuse transmission is not a source of polarization becomes less valid. The aerosol optical depth estimates at these shorter wavelengths are therefore not as good as those obtained at longer wavelengths (cf. Fig. 3.3). Since the surface contribution to the polarized reflectance is small at shorter wavelengths these problems can be overcome by iterative modeling of the polarized reflectance, that includes the effects of diffuse transmission, to finds the aerosol model that best matches all the measurements.

3.2 Over Oceans

In aerosol retrievals over the ocean the problem of non-uniqueness in retrieving aerosols properties from remotely sensed polarized radiances becomes more evident because the surface is darker and less variable than over land. This places greater expectations on the accuracy of aerosol retrievals over ocean and reveals that non-uniqueness, or the impact of erroneous assumptions, is a real problem in aerosol retrievals.

The data that are shown in this section were acquired over the ocean (several km from the coast) above the Santa Barbara Channel, California with the RSP mounted on an aircraft (3 km altitude, 50 m/s speed) and the scanner oriented along the direction of the aircraft ground track such that successive nadir views were one IFOV apart and the same point at the ground was seen from multiple viewing angles. Our study is focused on two RSP spectral channels centered at 0.865 and 2.250 μm because of the increased complexity of using shorter wavelength channels in coastal waters [9, 10]. We use the radiances and polarized radiances measured by the RSP to retrieve all parameters of the coarse and fine aerosol modes, including the spectral refractive index (m_λ), the effective radius (r_{eff}) and effective variance (v_{eff}) of the log normal size distribution, the contribution to the total spectral optical thickness (τ_λ), and the column number density of particles (N) in each mode. Our retrieval algorithm uses measurements at 2.250 μm to provide an estimate of the coarse mode properties under the assumption that the fine mode aerosol optical thickness at 2.250 μm is much smaller than that of the coarse mode. Once an estimate of the coarse mode properties has been obtained, it is used, together with the 0.865-μm measurements, to estimate the parameters of the fine mode. This initial guess is then used as the starting point in a non-linear iterative search, using the Levenberg-Marquardt method [11] coupled to vector radiative transfer calculations, which converges rapidly (3-5 iterations) to a solution that is consistent with all the measurements used in the fitting process, given their known uncertainties. A comparison between the optical depths measured by multi-filter rotating shadowband radiometers (MFRSRs) [12] and inferred from polarimetry for 14 October 1999 (Oxnard, CA) and 31 March 2000 (Goleta, CA) shows optical depth differences at 0.55μm of –0.01 and 0.008 respectively. Since the spectral slope of the inferred optical depth depends on the retrieved size distribution and since the shortest wavelength used in the RSP retrieval is 0.865 μm, the good fit over this spectral range is indicative of the quality of the size distribution retrieval [13].

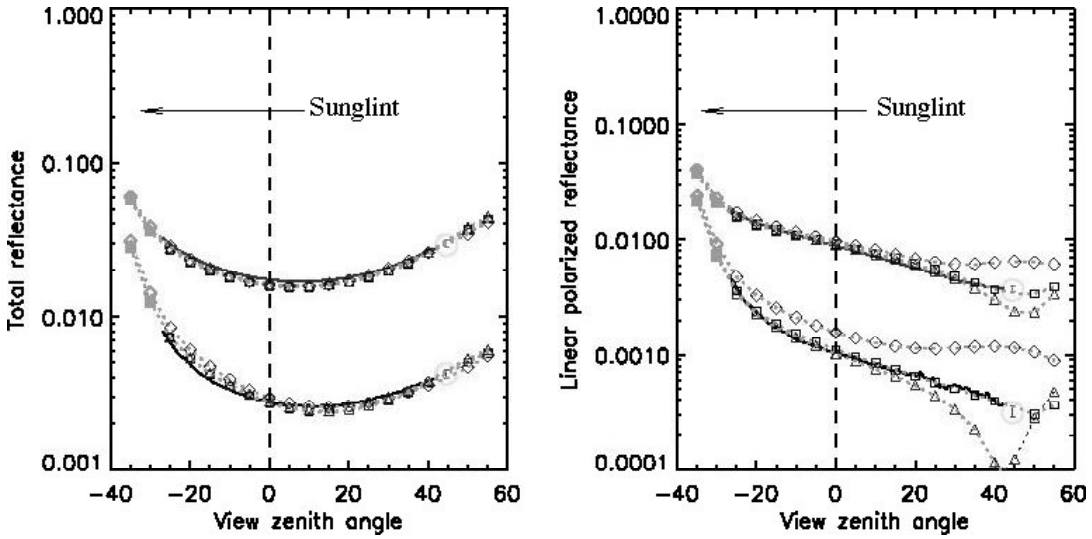

Figure 3.4. a) Reflectance and b) Polarized reflectance measurements at 865 and 2250 nm (upper and lower lines respectively). Symbols and dashed lines show model calculations in which the refractive index is increased by 0.03 shown by diamonds, or decreased by 0.09 shown by triangles. The reflectance can still be made to match the observations by changing the optical depth. It is only the polarized reflectance measurements that indicate which refractive index is appropriate.

These retrieved optical depths use the full angular range of RSP measurements and spectral bands at 865 and 2250 nm. The remarkable ability of the RSP measurements to constrain the aerosol model is demonstrated by calculations assuming a small increase (Δm = 0.03) in the coarse mode refractive index. Fig. 3.4a) shows that the resulting change in the total reflectance in both channels can be compensated for by a decrease in the coarse mode optical thickness (triangles). However, the fit to the polarized reflectance (triangles in Fig, 3.4b) becomes significantly worse, especially in the 2250 nm channel. In particular, polarization calculations at 2250 nm exhibit a neutral point at ~43° not seen in the measurements. In Figs. 3.4a) and 3.4b) it is shown that even larger errors in the refractive index (Δm = –0.09 indicated by diamonds) can be compensated by changing the optical thickness so that the intensity measurements are matched. The polarization measurements clearly rule this wrong solution out. These calculations illustrate that even multi-angle radiance measurements cannot retrieve the aerosol refractive index (and hence composition), and that assuming the refractive index *a priori* translates into significant errors in other retrieved parameters, e.g., optical thickness.

3.3 Clouds

3.3.1 Water Clouds

In Fig. 3.5 we show a model fit to measurements made over a thick stratus cloud deck. The model has a two layer cloud with larger particles in the upper layer and a haze between the cloud and the aircraft. A good fit can be obtained with a single layer cloud having the optical properties of the upper layer, but the fit is significantly improved by adding the complexity of an extra cloud and an extra haze layer. The need for a haze layer was identified purely from analysis of the polarization measurements, but its presence is confirmed in observer notes as the aircraft descended to cloud top.

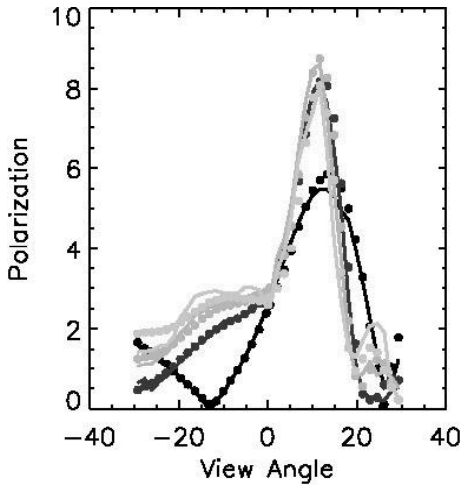

Figure 3.5. Comparison of model calculations and RSP measurements at 555, 678, 865 and 2250 nm (ordered top to bottom respectively at –15° view angle). The model uses a lower cloud layer with r_{eff}=5.0 µm, V_{eff}=0.10 and τ=12.5. The upper cloud layer has r_{eff}=7.4 µm, V_{eff}=0.078 and τ =3.0 and the haze layer consists of r_{eff}=2.75 µm, V_{eff}=0.10, τ =0.004. All optical depths are at a reference wavelength of 2250 nm.

The use of multi-angle polarization measurements to estimate cloud top properties can be contrasted with the use of single view angle radiances at absorbing and non-absorbing wavelengths that are principally sensitive to the effective radius of the particles [14]. The use of multiple angles and polarization allows for a robust retrieval of the effective radius and the effective variance of the particle size distribution. Sensitivity to haze above cloud top comes about because polarization of clouds away from the rainbow view angles is very low, so small polarizing haze particles above the cloud can be detected. It should be emphasized that the rainbow is a ubiquitous feature in polarization measurements of water clouds with the accuracy and precision provided by the RSP instrument. This is true even when there is no obvious rainbow feature in the intensity measurements, for example when clouds have a high optical depth.

3.3.2 Ice Clouds

The scattering of visible radiation by cirrus clouds depends principally on the optical depth of the clouds and on the shape of the ice crystals composing the clouds. This is because ice crystals are generally much larger than the dominant solar wavelengths, and the variation of their microphysical properties as a function of crystal size and wavelength is therefore quite weak. The inference of cirrus properties from the remote sensing measurements by instruments such as VIIRS therefore requires that assumptions about the crystal habit be made, or that the crystal habit be retrieved in order to have robust estimates of the required quantities, i.e., the particle size, optical depth and Ice Water Path (IWP). Incorrect assumptions about the crystal habit can cause large errors in the optical depth retrieved from solar reflectance measurements [15, 16], errors in the estimated particle size [17] and erroneous angular variations in the inferred albedo of the cirrus clouds [18]. RSP measurements can constrain crystal habit, reducing these uncertainties and providing better estimates of IWP.

3.3.3 Thin Cirrus Clouds

In the case of thin cirrus clouds it is desirable to be able to retrieve the aerosol loading and microphysical model for the atmosphere below the cirrus cloud. This requires that a spectral channel is provided that is predominantly sensitive to the upper troposphere and that the cirrus properties be retrieved using this band. At 1880 nm there is a strong water vapor band that ensures that surface features, low level clouds and boundary layer aerosols are not observed and the RSP instrument uses a spectral channel in this band to provide this capability. During the CRYSTAL-FACE field experiment sub-visible cirrus clouds were frequently observed: this type of cirrus is identified in RSP measurements by a negligible variation in the visible radiances and an order of magnitude increase in radiance in the band located at 1880 nm. These measurements provide sensitivity to cirrus clouds down to an optical depth of 0.01.

4. ATMOSPHERIC CORRECTION

4.1 Overview

Imaging and spectro-radiometric measurements made with remote sensing instruments are greatly affected by constituent gasses and aerosols in the optical viewing path. These change temporally, with range variations, illumination spectra, and viewing angles thereby affecting images and contaminating the spectral signatures of objects being observed remotely. Since such spatial and spectral "signature" data are used for detection and identification purposes, it becomes important to characterize the atmospheric absorption, scattering, and illumination of the optical path over which the data are collected. For example, radiance data sensed by a remote sensor must be corrected for atmospheric "modulation" to accurately derive **reflectance spectra** related to scene content and to identify the same objects of interest under different observation conditions.

As sensors become more sensitive and have higher spatial and spectral resolution capabilities, accurately knowing the existing optical path characteristics becomes more stringent. Small and spectrally narrow absorption features now discernable by advanced sensors, can confuse spectral signature data. Spectral characteristics that are very important to robustly identify targets are often masked by atmospheric path contaminants, especially spatially variable aerosols and water vapor. The detectable radiance spectra from a scene as sensed by overhead instrumentation will be different from the actual a-priori or measured reflectance spectra (ID discriminator) and will vary depending upon time of day, the viewing range, viewing angle, and atmospheric aerosol content, etc. Thus, it is important to know the actual characteristics of the atmospheric path within the field of view of a remote sensor at the time of measurement to derive target spectral information. This is particularly important for viewing in dusty conditions or for target ID with

battlefield smoke or chemical conditions, particularly as sensors become more sensitive and precisely calibrated. Typical post-flight data processing cannot accurately correct for such transitory aerosol line of sight contamination.

Generic data correction processes are inadequate to precisely correct for atmospheric path "noise" as needed to extract target "reflectance spectra" from scene radiance measurements as sensed by typical EOIR sensors. Typically atmospheric corrections are done via post-collection processing of recorded data, using ground based portable "ground-truth" photometric illumination measurements, and then applying generic atmospheric-model corrections via "standardized" software (MODTRAN, ACORN, and others) to derive the final "reflectance" hypercube data set. This process cannot precisely account for specific viewing path conditions; particularly where ground truth is not feasible or where long path aerosols are significant. The use of polarimetric measurements offer a means to obtain information from which new algorithms can be derived, and which in-turn can be used to up-date existing atmospheric modeling software packages. Current software algorithms are inadequate for such precision surveillance applications, thus there is a need for a significant improvement in generic atmospheric correction software, and secondarily a need to demonstrate a near real-time data collection regime via sensor integration processes using multiple instruments.

4.2 HyperSpecTIR (HST) Sensor

SpecTIR's HST sensor is flexible and offers in-flight programmability for various mission applications and on-the-fly changes in operating parameters. The sensor is equipped with a fast optical line-of-sight (LOS) steering system to accommodate data-collection from fast maneuvering tactical aircraft and RPVs. The HST design features an optimized optical system, gyro/image stabilization, and programmable operating systems. HST operational enhancements also include geolocation, geo-rectification, and turnkey real-time inflight reprogramming. Table 4.1 summarizes key characteristics and features of the HST.

The HST design is an evolution of the U.S. Navy HYDICE sensor with performance characteristics similar to the AVIRIS sensor deployed by JPL. The sensor utilizes a 2-D focal plane array with a whisk broom scan for image formation. The proprietary stabilization and scan technique facilitates stabilized imagery collection in turbulent and maneuvering conditions. The image formation approach provides accurate image geometry in the unprocessed image data. The programmable scan allows collections at a broad range of airspeeds and altitudes (GSDs) while still ensuring complete coverage (no under-sampling) of the target area. Real time GPS locations are included in the data stream allowing accurate geolocation of spatial pixels.

TABLE 4.1. HyperSpecTIR Sensor Summary

Parameter/ Component	Characteristics
Optics	Custom integral refractive (compensated telecentric)
Calibration	Complete system including all optics
Scanning/ Stabilization	Integrated high speed beam steering system
GIS/ Geolocation	Real time geolocation of ground pixels each frame
IFOV (Spatial Resolution)	1.0 milliradian (selectable in VNIR)
Swath Coverage	Programmable 0 to 1-radian (57°) (2-meter pixels at ~7000 ft altitude)
Spectrometer	Custom on-axis grating
Spectral Resolution	VNIR Programmable from 6nm to 12nm, SWIR ~ 8nm.
Spectral Range	450 to 2450 nanometers
Programm-ability	Fully programmable in real time; Number of Spectral Bands, Swath Width, V/H Comp., Integration Time (SNR)
Data Storage	Optical CD, DVD, Hard Disk Drive
Size	14 x 18 x 30 inches
Weight	150 pounds total in aircraft
Power	500W; Accommodates 28vdc or 115vac with uninterruptible power conditioning system

4.3 Approach To Atmospheric Correction

The radiance that is measured at the top of the atmosphere by a high spatial resolution (narrow field of view) instrument in a particular spectral channel, j, is given by the expression

$$I_j = \frac{\mu_0}{\pi \Delta\lambda_j} \int_{\Delta\lambda_j} r_j(\lambda) F_0(\lambda) R_{A-S}(\lambda) d\lambda \qquad (3)$$

in which r_j is the (properly normalized) spectral response in channel j, F_0 is the solar flux at the top of the atmosphere and $R_{A\text{-}S}$ is the reflectance of the atmosphere-surface system. The instrument spectral response, radiometric response and solar flux are important aspects of the final atmospheric correction and we briefly note the assumptions, or data sets that are used here. Instrument radiometric calibration is not discussed here except to note that radiometric accuracy is typically expected to be about 10% for hyper-spectral instruments [19, 20], although a 2% accuracy is claimed for the

improved AVIRIS instrument over the wavelength range 400-1800 nm [20]. The solar irradiance that is used here has a spectral irradiance distribution that is based on measurements by the SOLSPEC spectrometer [21] in the visible spectral domain (401 nm< λ < 874 nm) and a theoretical spectrum at longer wavelengths [22].

The simplest complete model of the reflectance of the atmosphere-surface system is

$$R_{A-S} = R_A + T_2 \frac{R_S}{1 - sR_S} \qquad (4)$$

where R_A is the atmospheric reflectance, T_2 is the two way transmission including both diffuse and direct beam transmission, R_S is the surface reflectance and s is the spherical albedo of the atmosphere when illuminated by the surface. It is important to note that when absorption is present and the atmosphere is vertically inhomogeneous the spherical albedo of the atmosphere is substantially different for illumination from below compared to when it is illuminated from above.

The principal problem in atmospheric correction is therefore the calculation of the atmospheric properties R_A, T_2 and is integrated over the instrument response so that the surface reflectance, which typically contains the spectral signature of interest, can be derived. The method that we use calculates the atmospheric scattering properties on a coarse spectral grid with a fixed set of absorption values that range over several orders of magnitude and with a vertical distribution consistent with line wing absorption. The scattering and absorption are then coupled by interpolating these scattering calculations to the required wavelength and integrating them over the absorption distribution provided by correlated *k*-distributions. A particular advantage of this approach is that because the scattering calculations and the resolution of the line absorption calculations are decoupled it is straightforward to perform calculations at any spectral resolution, provided *k* distributions are available at the required resolution, or line-by-line calculations from which such distributions can be calculated are available. The accuracy of this approach is generally excellent showing errors of less than 0.01 in the corrected reflectance in the center of absorption lines, for which the assumed vertical profile of gaseous opacity is incorrect. Comparisons of the "random" overlap method, that we use where there is absorption by multiple gases, with line-by-line calculations demonstrate that this

Figure 4.1. False black and white imagery of Pomona Golf Course using 450, 865 and 2250 nm bands.

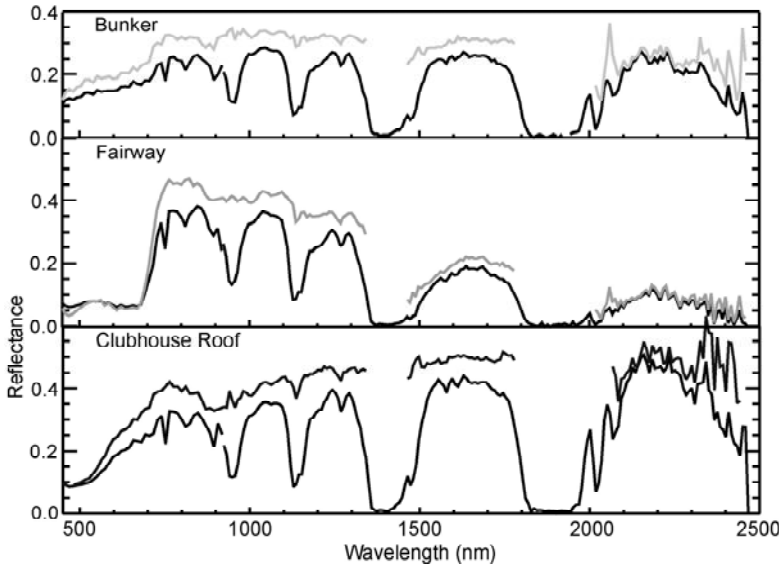

Figure 4.2. Sample atmospherically corrected spectra from the fairway and a bunker on the 18th hole and from the roof of the "19th hole".

approximation is adequate for 10 nm bandwidth instruments in the vicinity of 2000 nm where gaseous overlap between water vapor and carbon dioxide is a particular problem [23].

The examples of atmospherically corrected spectra shown in Figure 4.2 come from the HyperSpecTIR measurements taken over Pomona Golf Course on April 1st 2001 at 23:18 UTC, shown in Figure 4.1. The main source of difficulty in atmospheric correction of measurements such as these, when ground based measurements of the atmospheric state are not available, is the specification of the aerosol load and microphysical model and the amount of water vapor that is present. In Section 3 we described how measurements from the RSP instrument are used to estimate aerosol properties and it is these estimates that are used in the atmospheric correction process. In the examples presented here the water vapor amount is estimated from HyperSpecTIR measurements themselves [24]. The estimated water amount of 1.1 precipitable cm is consistent with that measured by a CIMEL instrument at JPL. It should be noted that no adjacency correction has been performed and that this is probably the cause of the "vegetation-like" increase in reflectance of the bunker spectrum at 680 nm. The aerosol optical depth at 550 nm is 0.355 and the bunkers are only a few pixels in size and so an adjacency correction should be performed to eliminate this structure. The structure of the corrected spectra at 2000 nm and at 2400 nm where carbon dioxide and methane absorption overlap with water vapor absorption is of concern and indicates that more line-by-line evaluations of the approach to mixing of gaseous absorption are required to evaluate the effect of this problem under varying water vapor loads and optical paths. In particular the data shown here were taken with a very high solar zenith angle of 55° which emphasizes any errors in the transmission, or reflection calculations.

5. CONCLUSIONS

In this paper we have described the RSP and HyperSpecTIR instrument and shown examples of data collected with these instruments. Both instruments are extremely robust and have been used in numerous data collects over the last four years. The RSP instrument has been used successfully at high altitude (58,000 feet) with more than 100 hours of high quality data being obtained. We have shown that the RSP instrument can be used to provide accurate estimates of aerosol loads and microphysical models over land surfaces and that over oceans the use of polarization measurement can eliminate ambiguities that are present in the estimate of aerosol properties using intensity only measurements.

The RSP aerosol retrievals have been used in a proprietary atmospheric correction code to correct measurements taken with the HyperSpecTIR instrument. The water vapor amount estimated from the HyperSpecTIR instrument is consistent with other measurements and the corrected spectra show plausible spectral reflectance distributions for sand, grass and man-made materials.

It remains to test the combined RSP/HyperSpecTIR payload on controlled targets with well characterized atmospheric constituents. This will allow the true limits and quality of the hyper-spectral measurements and the aerosol retrievals to be evaluated.

ACKNOWLEDGEMENTS

Some of the calculations presented in this paper were performed by Dr. Jacek Chowdhary (Figure 3.4) of Columbia University and by Dr. Makoto Sato (Figure 3.5) of SGT Inc. We would also like to acknowledge funding from the NASA Radiation Sciences Program and the NASA CRYSTAL-FACE field experiment.

REFERENCES

1: Cairns, B., L.D. Travis and E.E. Russell, The Research Scanning Polarimeter: Calibration and Ground-based measurements, *Proc. SPIE*, **3754**, 186-197, 1999.

2: Asner, G.P., Biophysical and biochemical sources of variability in canopy reflectance, *Remote Sens. Environ.,* **64**, 234-253, 1998.

3: Rondeaux, G. and M. Herman, Polarization of light reflected by crop canopies, *Remote Sens. Environ.*, **38**, 63-75, 1991.

4: Bréon, F-M, D. Tanré, P. Lecomte and M. Herman, Polarized reflectance of bare soils and vegetation: Measurements and models, *IEEE Trans. Geo. Rem. Sens*, **33**, 487-499, 1995.

5: Kaufman, Y. J. et. al., The MODIS 2.1µm channel - Correlation with visible reflectance for use in remote sensing of aerosol, *IEEE Trans. Geo. Rem. Sens*, **35**, 1286-1298, 1997.

6 Cairns, B., L.D. Travis and E.E. Russell, An analysis of polarization: Ground-based upward looking and aircraft/satellite based downward looking measurements. *Proc. SPIE,* **3220**, 103-114, 1997.

7: Hansen, J.E. and L.D. Travis, Light scattering in planetary atmospheres, *Space Sci. Rev.*, **16**, 527-610, 1974.

8: Hu, B.,W. Lucht and A.H. Strahler, The interrelationship of atmospheric correction of reflectances and surface BRDF retrieval: A sensitivity study, *IEEE Trans. Geo. Rem. Sens*, **37**, 724-738, 1999.

9: H.R. Gordon, 1997: Atmospheric Correction of Ocean Color Imagery in the Earth Observing System Era, *J. Geophys. Res.*, **102**, 17081-17106.

10: D. M. Tanre, et. Al. Remote Sensing of Aerosol Properties over Oceans Using the MODIS/EOS Spectral Radiances, *J. Geophys. Res.*, **102**, 16971-16998.

11: Ortega, J. M. and W. C. Reinbolt, *Iterative Solution of Nonlinear Equations in Several Variables*, Academic, New York, 1970.

12: Schmid, B., et al., Comparison of aerosol optical depth from four solar radiometers during the fall 1997 ARM intensive observation period, *Geophys. Res. Lett., 26*, 2725–2728, 1999.

13: Chowdhary, J., B. Cairns, M. Mishchenko, and L. Travis, 2001: Retrieval of aerosol properties over the ocean using multispectral and multiangle photopolarimetric measurements from the Research Scanning Polarimeter, *Geophys. Res. Lett*., **28**, 243-246.

14: T. Nakajima and M. D. King, 1996: "Determination of the optical thickness and effective particle radius of clouds from reflected solar radiation measurements. Part I: Theory," *J. Atmos. Sci.*, vol. 47, pp. 1878-1893.

15: Minnis, P., K.-N. Liou, and Y. Takano, 1993: Inference of cirrus cloud properties using satellite-observed visible and infrared radiances. I. Parameterization of radiance fields, *J. Atmos. Sci.* **50**, 1279–1304.

16: Mishchenko, M. I., W. B. Rossow, A. Macke and A. Lacis, 1996: Sensitivity of cirrus cloud albedo, bidirectional reflectance and optical thickness retrieval accuracy to ice-particle shape, *J. Geophys. Res.*, **101**, 16,973-16,986.

17: Rolland, G., K. N. Liou, M. D. King, S. C. Tsay and G. M. McFarquhar, 2000: Remote sensing of optical and microphysical properties of cirrus clouds using the Moderate Resolution Imaging Spectroradiometer channels: Methodology and sensitivity to physical assumptions, *J. Geophys. Res.*, **105**, 11,721-11,738.

18: C.-Labonnote, L., G. Brogniez, J.-C. Buriez and M. Doutriaux-Boucher, 2001: Polarized light scattering by inhomogeneous hexagonal mono-crystals: Validation with ADEOS-POLDER measurements. *J. Geophys. Res.*, **106**, 12,139-12,153.

19: Green, R. O., "Determination of the in-flight spectral and radiometric characteristics of the airborne visible/infrared imaging spectrometer (AVIRIS)," In *Imaging Spectrosocopy: Fundamentals and Prospective Applications*, ed. F. Toselli and J. Bodechtel (London: Kluwer Academic Publishers), pp. 103-123, 1992.

20: Chrien, T. G., R. O. Green, C. J. Chovit, M. L. Eastwood amd C. M. Sarture, "Calibration of the airborne visible/infrared imaging spectrometer in the laboratory," In *Summaries of the Sixth Annual JPL Airborne Earth Science Workshop, 4-8 March 1996* (Pasadena, CA: JPL Publications), pp.39-48.

21: Thuillier, G. M., Hersé, P.C. Simon, D. Labs, H. Mandel, D. Gillotay, and T. Foujols, "The visible solar spectral irradiance from 350 to 850 nm as measured by the SOLSPEC spectrometer during the ATLAS I mission," *Solar Phys.*, vol. 177, pp. 41-61, 1998.

22: Kurucz, R.L., "The solar spectrum," in *Solar Interior and Atmosphere*, A.N. Cox, W.C. Livingston, and M. S. Matthews (Eds.), The University of Arizona Press, Tucson, pp. 663-669, 1991.

23: Cairns, Brian, B. E. Carlson, R. Ying, A. A. Lacis and V. Oinas, Atmospheric correction and its application to an analysis of Hyperion data, *IEEE Trans.Geo. Rem. Sens.*, in press, 2003.

24: Gao, B. C. and A. F. H. Goetz, "Column atmospheric water vapor and vegetation liquid water retrievals from airborne imaging spectrometer data," *J. Geophys. Res.*, vol. 95, pp. 3549-3564, 1990.